

Occupancy of Nonannular Lipid Binding Sites on KcsA Greatly Increases the Stability of the Tetrameric Protein[†]

I. Triano, F. N. Barrera,[‡] M. L. Renart, M. L. Molina, G. Fernández-Ballester, J. A. Poveda, A. M. Fernández, J. A. Encinar, A. V. Ferrer-Montiel, D. Otzen,[§] and J. M. González-Ros*

Instituto de Biología Molecular y Celular, Universidad Miguel Hernández, Elche, 03202 Alicante, Spain

[‡]Present address: Department of Molecular Biophysics and Biochemistry, Yale University, New Haven, CT 06520-8114

[§]Interdisciplinary Nanoscience Center, Center for Insoluble Protein Structures (inSPIN), Department of Molecular Biology, University of Aarhus, DK-8000 Aarhus C, Denmark

Received March 10, 2010; Revised Manuscript Received May 12, 2010

ABSTRACT: KcsA, a homotetrameric potassium channel from prokaryotes, contains noncovalently bound lipids appearing in the X-ray crystallographic structure of the protein. The binding sites for such high-affinity lipids are referred to as “nonannular” sites, correspond to intersubunit protein domains, and bind preferentially anionic phospholipids. Here we used a thermal denaturation assay and detergent–phospholipid mixed micelles containing KcsA to study the effects of different phospholipids on protein stability. We found that anionic phospholipids stabilize greatly the tetrameric protein against irreversible, heat-induced unfolding and dissociation into subunits. This occurs in a phospholipid concentration-dependent manner, and phosphatidic acid species with acyl chain lengths ranging 14 to 18 carbon atoms are more efficient than similar phosphatidylglycerols in protecting the protein. A docking model of the KcsA–phospholipid complex suggests that the increased protein stability originates from the intersubunit nature of the binding sites and, thus, interaction of the phospholipid with such sites holds together adjacent subunits within the tetrameric protein. We also found that simpler amphiphiles, such as alkyl sulfates longer than 10 carbon atoms, also increase the protein stability to the same extent as anionic phospholipids, although at higher concentrations than the latter. Modeling the interaction of these simpler amphiphiles with KcsA and comparing it with that of anionic phospholipids serve to delineate the features of a hydrophobic pocket in the nonannular sites. Such pocket is predicted to comprise residues from the M2 transmembrane segment of a subunit and from the pore helix of the adjacent subunit and seems most relevant to protein stabilization.

Since the elucidation of the high-resolution, X-ray structure of KcsA¹ (1–3), this prokaryotic potassium channel from the Gram-positive soil bacterium *Streptomyces lividans* (4) has become the experimental model system of choice in many ion channel and membrane protein studies. The crystal structure of KcsA shows that the protein is arranged as a homotetramer with subunits of 160 amino acids, each comprising N- and C-terminal cytoplasmic domains and two transmembrane α -helices, TM1 and TM2, connected by a short helix and a P-loop containing the characteristic TVGYG sequence of the selectivity filter in potassium channels.

A further examination of the KcsA crystal structure reveals that it contains noncovalently bound lipid (2, 5), which was initially modeled as diacylglycerol. However, since phosphatidylglycerol (PG) was detected in detergent-solubilized KcsA at a ratio of 0.7 molecule per KcsA monomer (5), it was assumed that the protein-bound lipid was PG with the phosphoglycerol head-group too mobile to be solved in the X-ray structure. This identity was later confirmed through mass spectrometry experiments, which also indicated that KcsA prefers to bind PG rather than phosphatidylcholine (PC) (6). The crystallographic evidence and other studies (7) conclude that the PG binding sites on the KcsA protein have the features of the so-called “nonannular” lipid binding sites (8). Thus, the *sn*-1 acyl chain of each PG appears bound into a deep cleft on the protein surface, between TM1 and TM2 of two adjacent KcsA monomers, while the *sn*-2 chain binds more peripherally (2). The PG negatively charged polar head-group is expected to interact with nearby positively charged residues, such as R64 or R89. This latter interaction seems not to be very specific as there are only minor differences in the affinities of different negatively charged phospholipids for binding to KcsA (7, 9, 10). Lipids bound to “nonannular” sites of different membrane proteins have been documented in several instances and are believed to play important roles in modulating relevant protein features ranging from their correct folding to their optimal activity (11, 12). In KcsA in particular, such sites can

[†]Supported by grants from the Spanish MICINN BFU2008-00602 and BFU2009-08346 and Consolider-Ingenio 2010 CDS2008-00005. D.O. is supported by the Danish Research Foundation via inSPIN. I.T. was partly supported by a predoctoral fellowship from the Ministerio de Educación of Spain.

*To whom correspondence should be addressed. Phone: +34 96 6658757. Fax: +34 96 6658758. E-mail: gonzalez.ros@umh.es.

¹Abbreviations: KcsA, potassium channel from *Streptomyces lividans*; DDM, dodecyl β -D-maltoside; SDS–PAGE, polyacrylamide gel electrophoresis in the presence of sodium dodecyl sulfate; CD, circular dichroism; DOPA, 1,2-dioleoyl-*sn*-glycero-3-phosphate; DOPC, 1,2-dioleoyl-*sn*-glycero-3-phosphocholine; DOPE, 1,2-dioleoyl-*sn*-glycero-3-phosphoethanolamine; DOPG, 1,2-*sn*-glycero-3-[phospho-*rac*-(1-glycerol)]; egg PG, L- α -phosphatidylglycerol (egg, chicken); egg PA, L- α -phosphatidic acid (egg, chicken); PG, phosphatidylglycerol; PC, phosphatidylcholine; PA, phosphatidic acid; T_m , midpoint denaturation temperature; ΔH_{D-N} , enthalpy change of denaturation; ΔC_p , change in heat capacity.

be specifically occupied by anionic phospholipids (7, 10), and their occupancy seems to be important for channel function (13, 14). Also, *in vitro* folding experiments using trifluoroethanol (TFE) as a denaturant have shown that the unfolded monomers to folded KcsA tetramer transition occurs fully reversibly, including recovery of channel function, only when in the presence of specific lipids (15). Furthermore, it has been shown that phosphatidylethanolamine–phosphatidylglycerol mixtures were optimal for efficient KcsA membrane association and tetramerization using a coupled *in vitro* transcription–translation system (16), demonstrating the importance of membrane lipid composition for KcsA assembly. Therefore, the fact that bound lipids modulate the folding and oligomerization state of the protein, as well as its ion channel activity, makes it extremely interesting to study the interactions involved.

Here we report on the effects of different lipids on the stability of the KcsA tetramer in a mixed micelle system containing both the probe lipids and excess detergent (dodecyl β -D-maltoside, DDM). Our observations, based on a thermal denaturation assay, indicate that all anionic phospholipids tested, regardless of their polar headgroup and in a concentration-dependent manner, strongly stabilize the tetrameric KcsA protein against thermal denaturation into unfolded monomers, which is an irreversible process. Strikingly, we also observed that a similar protein stabilization could be obtained by negatively charged alkyl sulfates, such as sodium dodecyl sulfate (SDS), suggesting that these latter molecules also bind to the “nonannular” lipid binding sites on KcsA.

MATERIALS AND METHODS

Protein Expression and Purification. Expression of the wild-type KcsA protein with an added N-terminal hexahistidine tag in *Escherichia coli* M15 (pRep4) cells and its purification by affinity chromatography on a Ni^{2+} -Sepharose (GE Healthcare) column were carried out as reported previously (17), except that the final buffer used with the stock of purified protein was 20 mM Hepes (Sigma-Aldrich), pH 7.0, containing 100 mM NaCl (Merck) and 5 mM DDM (Calbiochem). The sample was dialyzed to eliminate the imidazole used to elute the protein from the column. The protein concentration was routinely determined from the absorbance at 280 nm, using a molar extinction coefficient of $44808 \text{ M}^{-1} \cdot \text{cm}^{-1}$ for the KcsA monomer. This molar extinction coefficient was calculated from samples in which the KcsA concentration was determined by quantitative amino acid analysis (15). KcsA concentration values in this report are always given in terms of KcsA monomers.

Fluorescence Monitoring of Thermal Denaturation. Thermal denaturation of KcsA was carried out in a Varian Cary Eclipse spectrofluorometer at a temperature up-scan rate of $0.6 \text{ }^\circ\text{C}/\text{min}$. Experiments were performed in a 1 cm quartz cuvette with a final KcsA concentration of $0.5 \mu\text{M}$ solubilized in a buffer containing 20 mM Hepes, pH 7.0, 100 mM NaCl, and 1 mM DDM, supplemented with increasing concentrations of the corresponding phospholipids (Avanti Polar Lipids) or *n*-alkyl sulfates (Sigma-Aldrich). The excitation wavelength was 280 nm, and the fluorescence emission was recorded at 340 nm. Slit widths for excitation and emission were 2.5 and 10 nm, respectively, and the integration time was 3 s. Simultaneously, fluorescence emission spectra were taken at selected temperatures during the heating scan, between 300 and 400 nm, at a $60 \text{ nm}/\text{min}$ scan rate and using a 1 nm resolution, with an averaging of three spectra

for each sample and temperature. The midpoint temperature of dissociation and unfolding of the tetramer (T_m) was calculated from the thermal denaturation curve by fitting the data to a two-state unfolding model, assuming a linear dependence of the pre- and posttransition baselines on temperature (18):

$$F_{340} = \frac{\alpha_N + \beta_N(T - 298) + (\alpha_D + \beta_D(T - 298))e^{\frac{-\Delta H_{D-N}}{R}\left(\frac{1}{T} - \frac{1}{T_m}\right)}}{1 + e^{\frac{-\Delta H_{D-N}}{R}\left(\frac{1}{T} - \frac{1}{T_m}\right)}} \quad (1)$$

where F_{340} is the observed fluorescence emission at a given temperature, α_N and α_D are the intrinsic fluorescence of the native and denatured state, respectively, at 298 K, β_N and β_D are the slopes of the native and denatured state baselines, respectively, T is the temperature, T_m is the midpoint denaturation temperature in kelvin (we use the term t_m to refer to the midpoint denaturation temperature in degrees centigrade), ΔH_{D-N} is the enthalpy change of denaturation, which is related to the slope of the curve at T_m , and R is the gas constant. Kaleida Graph (Synergy Software) was used for the fittings.

Circular Dichroism (CD) Monitoring of Thermal Unfolding. Far-UV CD monitoring of the thermal denaturation of KcsA was performed to assess the loss of the protein secondary structure as the temperature is increased. Ellipticity at 222 nm was taken on a Jasco J810 spectropolarimeter at a temperature up-scan rate of $0.6 \text{ }^\circ\text{C}/\text{min}$. The samples were thermostated with a Jasco Peltier system and contained into 0.1 cm path-length quartz cuvettes. Simultaneously, CD spectra were taken at selected temperatures during the heating scan, between 205 and 250 nm at a $50 \text{ nm}/\text{min}$ scan rate and using a 0.2 nm resolution, with an accumulation of six spectra for each sample and temperature. The final concentration of KcsA in the CD measurements was $3 \mu\text{M}$.

The mean residue ellipticity, $[\theta]$, was calculated as

$$[\theta] = \frac{\theta \text{MW}}{10lc(N-1)} \quad (2)$$

where θ is the measured ellipticity in degrees, MW is the molecular mass of the KcsA monomer (Da), l is the path length (cm), c is the KcsA concentration (g/mL), and N is the number of amino acid residues (19).

Occasionally, CD thermal denaturation curves were also used in addition to the fluorescence data to estimate the midpoint denaturation temperature t_m and the enthalpy change of denaturation ΔH_{D-N} (18).

SDS-PAGE. KcsA solutions ($3 \mu\text{M}$) in 20 mM Hepes, pH 7.0, 100 mM NaCl, and 1 mM DDM were submitted to the heating routine described above in the Varian Cary Eclipse spectrofluorometer, and aliquots containing $1.3 \mu\text{g}$ of protein were withdrawn at selected temperatures and mixed with electrophoresis sample buffer (20). Samples were cooled on ice until they were run in 13.5% SDS-PAGE. Protein bands were visualized after Coomassie Brilliant Blue staining.

Modeling of KcsA. KcsA–lipid complexes were built using the KcsA–Fab template in low K^+ (high Na^+) concentration having cocrystallized lipid structures (2) (PDB code 1K4D). The partial lipid structures in the crystal were used as a scaffold to build entire lipid molecules with different polar headgroups.

Molecules were edited and reconstructed with the general purpose molecular modeling software Yasara (21, 22). The resulting KcsA–lipid complexes were used for docking purposes. The program performs a simulated annealing minimization of the complexes, which moves the structure to a nearby stable energy minimum, by using the implemented AMBER 99 force field (23). The binding energy is obtained by calculating the energy at infinite distance between the ligand and the KcsA oligomer and subtracting the energy of the whole complex. The more positive the binding energy, the more favorable the interaction is in the context of the force field. A local docking procedure was accomplished with AutoDock 4 (24), where a total of 100 flexible or rigid docking runs are set and clustered around the lipid binding site, and the best binding energy complex in each cluster is stored and analyzed. Figures were drawn with Pymol (DeLano Scientific, Palo Alto, CA; <http://www.pymol.org>).

RESULTS

Thermal Denaturation of Solubilized KcsA Is a Cooperative Process. Figure 1A shows intrinsic fluorescence monitoring of the thermal denaturation of purified KcsA in detergent solution as the temperature increases at a constant heating rate. In the lower temperature range (the native state baseline), the protein intrinsic fluorescence decreases in a linear fashion with temperature in accordance with the general increase in quenching of fluorescence with temperature (25), then goes into a sigmoidal-like region with a steeper slope, and finally, in the higher temperature range (the denatured state baseline), returns to a linear decrease with a slope different from that seen at lower temperatures. The decrease in fluorescence intensity with increasing temperature is accompanied by a red spectral shift in the intensity-weighted average emission wavelength from approximately 339 nm at 25 °C to 348 nm at 95 °C. Finally, it should be noticed that the sigmoidal-like event in the thermal denaturation curves completely disappears from a second heating scan of thermally denatured, recooled samples, indicating that thermal denaturation of KcsA is an irreversible process (data not shown).

When we used far-UV CD measurements to follow the loss of secondary structure with temperature, we observed that heating induces the irreversible unfolding of the protein, which loses more than 70% of its characteristic ellipticity at 222 nm, as well as all other features of the typical spectrum of α -helical proteins. As in the fluorescence measurements, the loss of ellipticity is linear in the lower temperature range, then follows a sigmoidal-like pattern, and finally becomes linear again at higher temperatures (Figure 1B). We have no proper explanation for the sloping baselines in the native and unfolded regions of the thermal scan, but note that this is a common phenomenon observed both in membrane proteins (18, 26) and in water-soluble proteins (27).

SDS–PAGE analysis of KcsA samples taken at different temperatures (Figure 1C) reveals that the heat-induced process seen by fluorescence and CD includes the irreversible transition from the well-known, folded homotetramer accounting for most of the detergent-solubilized KcsA protein obtained from the *E. coli* expression system (17) to partly unfolded monomers. Such monomers further aggregate to yield protein material unable to enter into the electrophoretic gel.

The midpoint temperatures (t_m) for all the above processes, i.e., the fluorescence and CD changes as well as the dissociation into monomers of the tetrameric KcsA observed by SDS–PAGE, are practically identical within experimental error (see

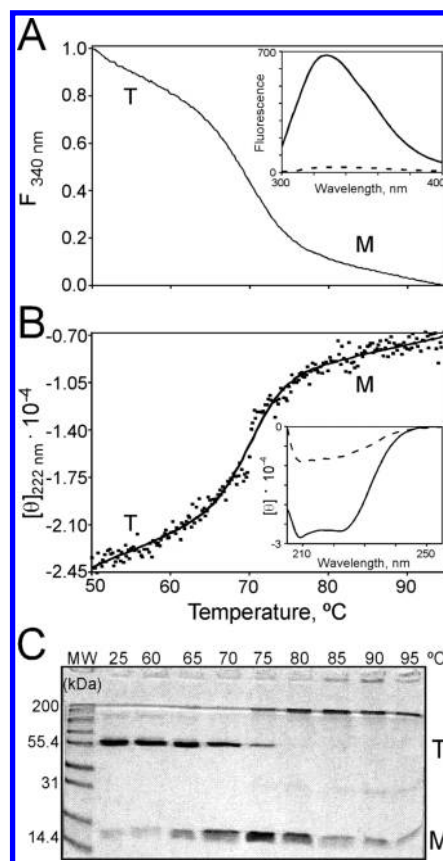


FIGURE 1: Panel A illustrates thermal denaturation of KcsA monitored by intrinsic fluorescence. The experimental trace shows the changes in the fluorescence emission at 340 nm (in arbitrary units) upon excitation at 280 nm, as the temperature is increased. KcsA samples (0.5 μ M) were in a 20 mM HEPES buffer, pH 7.0, containing 100 mM NaCl and 1 mM DDM. The t_m estimated from four different experiments was 70.7 ± 0.6 °C. The inset shows the fluorescence spectrum obtained at 50 °C (solid line) and at 95 °C (dashed line). T and M within the figure indicate the regions of the thermal denaturation curves corresponding to KcsA tetramers and monomers, respectively. Panel B illustrates the CD monitoring of thermal denaturation of a 3 μ M solution of KcsA in the buffer from above. The experimental values of the mean residue ellipticity at 222 nm in units of $\text{deg} \cdot \text{cm}^2 \cdot \text{dmol}^{-1}$ appear as dots within the figure. The fitting of such data to eq 1 (see Materials and Methods section) is also shown. The t_m estimated from two different experiments was 72 ± 2 °C. The inset shows circular dichroism spectra at 50 °C (solid line) and at 95 °C (dashed line). Panel C shows a SDS–PAGE gel (13.5%) used in electrophoretic monitoring of the thermal denaturation of a 3 μ M KcsA solution in the same buffer from above. Heating and processing of the samples for electrophoresis are as indicated under Materials and Methods. The t_m estimated from densitometry of two different gels was 72.7 ± 0.5 °C.

legend to Figure 1), suggesting that the dissociation of the tetramer and the loss of secondary and tertiary protein structure occur concomitantly.

It should be noted here that the characteristic t_m value for the heat-induced dissociation and unfolding process is strongly dependent on the type and concentration of ions present in the buffer. This is due to the role of certain ions on stabilizing the KcsA protein (28, 29). In particular, the presence of potassium ions at concentrations above 10–15 mM increases the t_m to values near the boiling point of water, which would prevent us from acquiring a good baseline for the denatured state in our aqueous samples. Therefore, we carried out these measurements in a sodium buffer in which the t_m 's of the DDM-solubilized KcsA under the different experimental conditions used in this

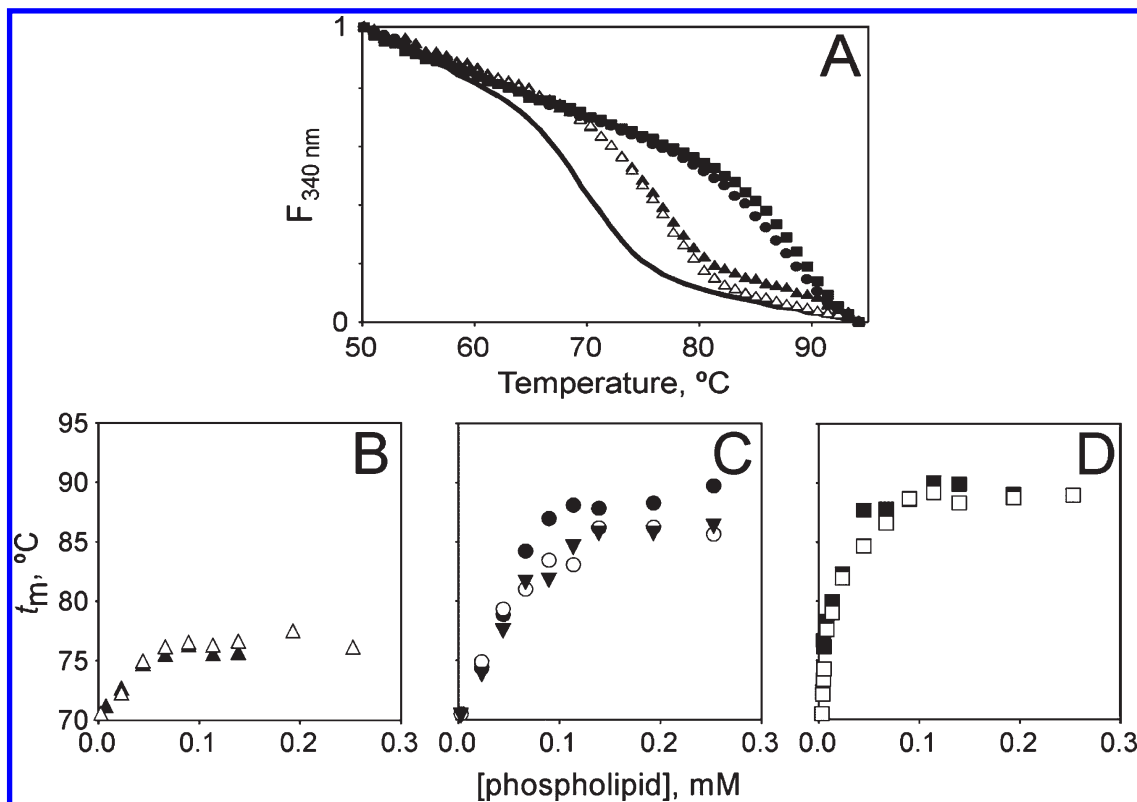


FIGURE 2: Fluorescence monitoring of thermal denaturation of KcsA in mixed micelles of DDM and different phospholipids. Panel A shows representative thermal denaturation curves of KcsA at $0.5 \mu\text{M}$ in 20 mM Hepes, pH 7.0, containing 100 mM NaCl and 1 mM DDM, in the absence of added phospholipids (control, solid line) and in the presence of the same concentration (0.1 mM) of DOPE (▲), DOPC (△), DOPG (●), or DOPA (■) within the mixed micelles to facilitate comparison. Panels B–D show the dependence of the t_m values on the concentration of different phospholipids, including the zwitterionic DOPE (▲) and DOPC (△) (panel B), as well as the anionic PG-derived phospholipids DOPG (●), DMPG (○), and egg PG (▼) (panel C) and PA-derived phospholipids DOPA (■) and egg PA (□) (panel D).

work are within a lower temperature range, more amenable for our experimental settings.

Anionic Phospholipids Preferentially Stabilize KcsA. The effects of the different phospholipids on the stability of KcsA have been assessed in thermal denaturation experiments using mixed micelles containing the lipid to be tested and excess detergent (DDM) to keep the samples solubilized. Figure 2 shows that all phospholipids tested increased the KcsA thermal stability in a concentration-dependent manner in the presence of 1 mM DDM, showing saturation at around 0.1 mM lipid. This corresponds to a lipid to detergent molar fraction of ~ 0.1 . However, anionic phospholipids were much more efficient than zwitterionic phospholipids in increasing the protein's thermal stability. Indeed, t_m values undergo a remarkable $\sim 20^\circ\text{C}$ increase in the presence of the anionic phospholipids PG (Figure 2C) and PA (Figure 2D), versus the more modest $\sim 7^\circ\text{C}$ increase in t_m produced by the zwitterionic phospholipids used in this study (Figure 2B). Interestingly, there were no apparent differences in the effects of the different zwitterionic phospholipids tested (PC and PE species) on the protein's thermal stability. Conversely, the effects on the t_m of the anionic phospholipids exhibited a clearly different concentration dependence, and indeed, the affinity of the PA species for KcsA seems significantly higher than that of the PG species, regardless of their fatty acyl components.

Effects of Alkyl Sulfates on Thermal Stability of KcsA Indicate That 10–14 Carbon Atom Long Alkyl Chains Can Be Accommodated in the Nonannular Lipid Binding Site. Linear alkyl sulfates of different chain lengths were also included in these studies as simpler model amphiphiles exhibiting some of

the main features of the anionic phospholipids from above, i.e., a negatively charged group at the end of a hydrophobic moiety. Figure 3 shows that alkyl sulfates with short-chain lengths (6–8 carbon atoms) have negligible effects on protein stability. However, just as the anionic phospholipids, alkyl sulfates beyond a certain chain length are also able to stabilize the KcsA protein against thermal dissociation and unfolding in a concentration-dependent manner. Indeed, the efficiency of the longer amphiphiles (12 and 14 carbon atoms) is such that the thermal stabilization phenomenon, although achieved at higher concentrations, is almost identical to that seen for the anionic phospholipids in terms of the increase in t_m .

Thermodynamics of Unfolding Suggest Significant Interactions of Alkyl Sulfates with KcsA in the Denatured State. Fitting the thermal denaturation curves for unfolding of KcsA in the presence of alkyl sulfates provides not only the midpoint of denaturation t_m but also the associated enthalpy of denaturation ΔH_{D-N} . Given that denaturation is irreversible and involves dissociation from tetramer to monomer, a detailed quantitative analysis should be approached with caution. Nevertheless, initial stages of denaturation generally approach equilibrium conditions. Furthermore, even as irreversible phenomena, the unfolding enthalpies can be viewed as activation enthalpies which by themselves are subject to the same types of thermodynamic analyses as conventional equilibrium enthalpies (30). As all the thermal scans are performed under similar conditions and presumably with the same level of irreversibility, we feel justified in carrying out a comparison of the enthalpies, which indeed provides an interesting trend. Conventionally, the slope of the

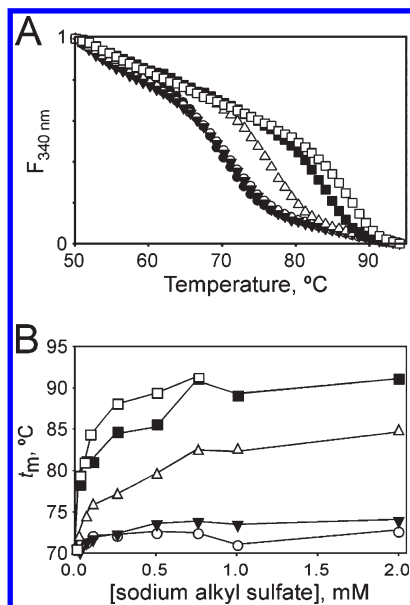


FIGURE 3: Thermal denaturation of KcsA in mixed micelles of DDM and different sodium alkyl sulfates. Panel A shows fluorescence monitoring of thermal denaturation of KcsA (0.5 μ M) in 20 mM Hepes, pH 7.0, containing 100 mM NaCl and 1 mM DDM, in the absence of alkyl sulfates (\bullet , control) and in the presence of a fixed concentration (0.25 mM) of sodium alkyl sulfates with a different chain length: hexyl (\circ), octyl (\blacktriangledown), decyl (Δ), dodecyl (\blacksquare), and tetradecyl (\square) within the mixed micelles. Panel B shows the concentration dependence of the t_m values obtained for the denaturation of KcsA in the presence of increasing concentrations of the different sodium alkyl sulfates from above.

plot of ΔH_{D-N} versus t_m is interpreted as the change in heat capacity (ΔC_p) associated with denaturation (31). ΔC_p is normally positive for globular proteins. The reason for this is not completely clear, but a possible explanation is that thermal denaturation leads to increased solvent exposure of contiguous hydrophobic regions. At the interface between water and these hydrophobic regions, the water molecules assume a structure similar to the interface between liquid and vapor (32). This leads to increased formation of “low angle hydrogen bonds” with larger energy fluctuations than the conventional “high angle” bonds, which in turn leads to a higher heat capacity than bulk water (33). The situation is more complex for membrane proteins solubilized by amphiphilic molecules and liganded to alkyl sulfates. A plot of ΔH_{D-N} versus t_m for KcsA shows an essentially linear correlation for all alkyl sulfates C8–C14 (Figure 4A) with the expected positive values of ΔC_p , but ΔC_p decreases with increasing alkyl length (Figure 4B). This decrease may be interpreted in two different ways: (a) increased compaction of the denatured state in the presence of longer alkyl chains, which have higher affinities for KcsA than the short-chain alkyl sulfates, or (b) aggregation-linked unfolding, which increases the steepness of the unfolding transition and thus increases the apparent ΔH_{D-N} . This latter effect may be expected if the shorter alkyl chains do not shield the hydrophobic parts of denatured KcsA as well as the longer chains. We acknowledge the limitations in the interpretation of these data. However, note that both scenarios envisage binding of alkyl sulfates to the denatured state with various affinities and thus complement the more straightforward conclusions obtained from the analysis of the variation in t_m with alkyl chain lengths.

Modeling Interactions at Nonannular Binding Sites of KcsA. Figure 5A shows the starting structure resulting from

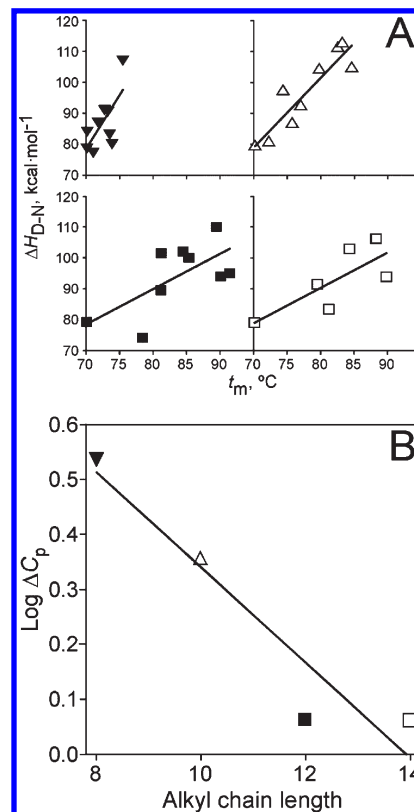


FIGURE 4: Apparent enthalpy of unfolding (ΔH_{D-N}) versus t_m plots for the unfolding of KcsA in the presence of alkyl sulfates of different chain lengths. ΔH_{D-N} and t_m parameters were obtained from fitting the thermal denaturation curves to eq 1. Panel A shows the plots corresponding to octyl, decyl, dodecyl, and tetradecyl sulfates. The slopes of such plots (correlation coefficients, R^2 , ranging from 0.45 to 0.84) yielded ΔC_p . Panel B shows the dependence of the logarithm of ΔC_p versus the chain length in terms of carbon atoms. Symbols used are as in Figure 3.

building the KcsA–lipid complexes based on the existing crystallographic data, prior to local docking. The figure shows four DOPG molecules bound to nonannular sites on the protein. Panels B and C of Figure 5 show in detail the resulting interactions predicted from local docking of a DOPG molecule into one of the intersubunit nonannular sites of KcsA. A first important observation is that DOPG after the docking procedure conforms quite precisely to the partial lipid structure seen in the protein crystal. Moreover, the polar headgroup of the phospholipid, which is not seen in the crystal, points toward the charged groups near the extracellular surface in the nonannular cleft and exhibits conformational flexibility. Indeed, both the *sn*-1 carbonyl ester of DOPG and the hydroxyl groups in the polar head can be predictably hydrogen bonded to either R89 in one subunit and/or R64 and T61 in the adjacent subunit. As to the *sn*-1 acyl chain, the prediction is that it first goes through a gorge defined mainly by the side chain of L86 of one subunit and the side chain of P63 in the adjacent subunit (Figure 5B) and then interacts with multiple hydrophobic side chains within a hydrophobic pocket contributed mainly by R89, C90, V93, V94, and V97, all belonging to the M2 transmembrane segment of one subunit, plus L66 in the pore helix of the adjacent subunit (Figure 5C). On the other hand, the *sn*-2 acyl chain is expected to run first over the surface of one of the protein subunits, and then it poses its methyl terminal half into a hydrophobic cleft on the surface of the adjacent subunit (Figure 5C). Local docking of DOPA instead of DOPG results in similar predictions, except that an additional

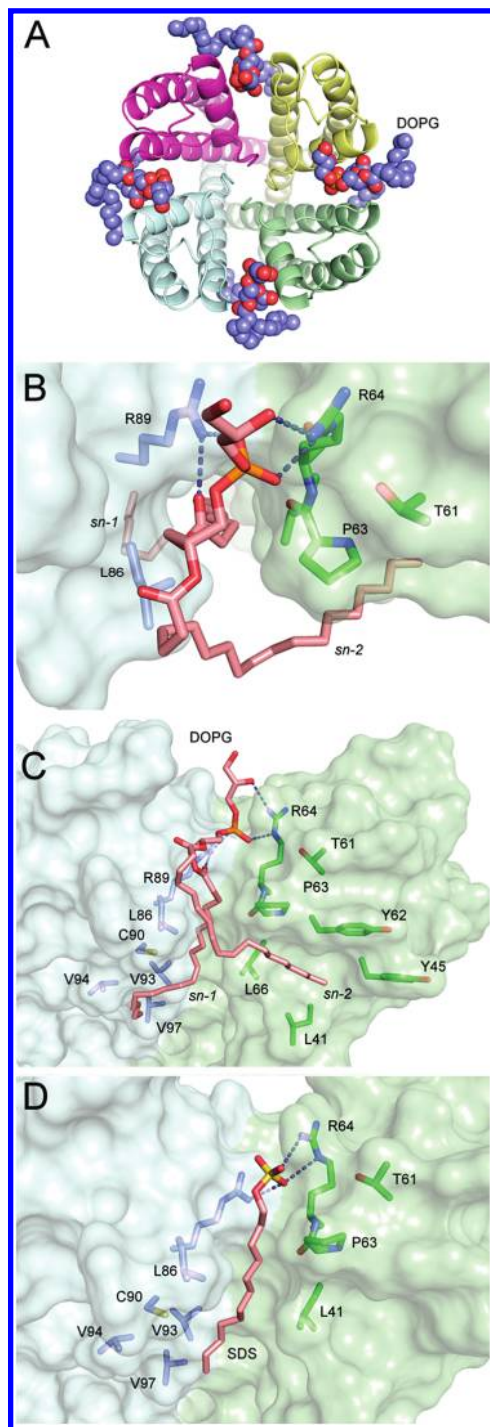


FIGURE 5: Molecular models of the intersubunit, nonannular lipid binding site of KcsA. Panel A shows a top view (normal to the membrane plane) of the starting crystallographic structure obtained from PDB code 1K4D (2) prior to local docking. Four DOPG molecules (carbon atoms colored in blue) have been drawn bound to the nonannular protein sites. Such DOPG molecules were built by using the partial lipid structure appearing in the protein crystal as a scaffold. Panels B and C show top and side views, respectively, of the results from local docking of a DOPG molecule into one of the intersubunit nonannular sites. Adjacent KcsA protein subunits are colored in light blue and green. The corresponding one letter code and numbering in the KcsA sequence for the main amino acid residues involved in the interaction with the phospholipid have been included. The *sn*-1 and *sn*-2 acyl chains of DOPG have been also identified. Panel D shows a side view of the results from docking an SDS molecule into the same nonannular lipid binding site. Hydrogen bonds have been indicated by dark blue dashed lines.

hydrogen bond with the cationic amino acid residues is established when DOPA is in the dianionic form. This further confirms that anionic phospholipids in their interaction with the protein are holding together adjacent subunits within the tetrameric KcsA structure.

Figure 5D shows the results of local docking of SDS, one of the long-chain alkyl sulfates used in this work, into the same nonannular site of KcsA where anionic phospholipids bind. The rationale for doing such docking is that long-chain alkyl sulfates and anionic phospholipids have almost identical quantitative effects on increasing the protein thermal stability, and therefore, it is reasonable to assume that they both bind to the same protein sites. The docking shows that, indeed, SDS is also predicted to establish interactions with residues belonging to adjacent KcsA subunits, which is consistent with the observed tetramer stabilization. In particular, the sulfate group hydrogen bonds to R89 and R64 or, alternatively, to R64 and T61 (not shown), indicating flexibility of the sulfate head moiety. As to the alkyl chain, it interacts similarly to the *sn*-1 acyl chain of the anionic phospholipids, although less deeply, going first through the L86 and P63 gorge and then into the intersubunit hydrophobic pocket.

While providing a reasonable explanation to the observed protein stabilization phenomena, the docking model might also be testable. Work is in progress in our laboratory to prepare point mutations of the channel protein to explore the significance of individual amino acid residues predictably involved in the interaction with either the high-affinity phospholipids or the alkyl sulfate amphiphiles.

DISCUSSION

The presence of lipid molecules tightly (but noncovalently) bound to membrane proteins has been documented in several instances (8, 11). Tight binding prevents these lipids from dissociating appreciably from the protein by treatments such as detergent solubilization, and indeed, they cocrystallize with the protein and have been seen occasionally in the high resolution, X-ray structures. The binding sites for these lipids, referred to as nonannular sites, have been suggested to correspond to clefts or grooves between transmembrane helices or at protein–protein interfaces (34, 35). Lipids able to bind to those sites are usually anionic phospholipids or cholesterol and seemingly correspond to the same lipids required for function by many membrane proteins. In KcsA in particular, the tightly bound anionic lipid that copurifies with the protein is PG. Nonetheless, the nonannular sites on the protein can bind other anionic phospholipids as well (7, 10), and their occupancy seems to be important for KcsA structure and function (13–16).

We have used here a thermal denaturation assay to study in more detail the interactions involved in binding to the nonannular sites in KcsA. The assay is carried out using purified, detergent-solubilized KcsA, which provides a fairly homogeneous sample as the detergent diminishes intermolecular clustering and causes ~90% of the protein to be present as the well-known tetramer of four identical subunits (36). Furthermore, these samples are fully amenable for fluorescence or CD spectroscopic monitoring. In particular, we found the intrinsic protein fluorescence particularly valuable for our purposes, not only because of its sensitivity, which allows use of low protein concentrations, but also because the Trp residues in KcsA are exclusively located at both ends of the transmembrane helical

segments of the protein, defining the extracellular (W67, W68, and W87) and the intracellular (W26 and W113) lipid–water interfaces, respectively, which makes Trp fluorescence very sensitive to conformational rearrangements.

Our results indicate that KcsA in detergent micelles and sodium buffer undergoes an irreversible, cooperative process of thermal denaturation, which includes dissociation of the tetramer into monomers and protein unfolding. Such unfolding and tetramer dissociation processes seem to occur simultaneously, as indicated by the practically identical midpoint temperature (t_m) values derived from either the fluorescence, electrophoretic, or CD data. It should be noted, however, that the protein concentrations in the fluorescence measurements were lower than those used in the CD and SDS–PAGE experiments, and therefore, such a comparison cannot be made in strict terms. Nonetheless, the concomitant occurrence of dissociation and unfolding are supported by experiments of chemical (TFE) denaturation of the KcsA protein (20).

KcsA has annular and nonannular lipid binding sites at its membrane-exposed surface. Annular sites bind the annular shell of “solvent” lipids, with little or no headgroup selectivity. In contrast, nonannular sites of KcsA bind only anionic phospholipids (9, 10), and therefore, the strong stabilization effect seen in our experiments in the presence of either PA or PG must arise from their interaction with the nonannular sites of the protein. Likewise, the smaller effect on the t_m observed for zwitterionic phospholipids is likely to account for their interaction with annular sites. The electrostatic interaction between anionic headgroups in the phospholipid and positively charged amino acid residues constitutes the basis for selective binding to the nonannular sites (7, 10). In this respect, the higher affinity observed for PA in increasing the protein’s t_m could be ascribed to the ability of PA to increase its negative charge (to become a dianionic species) when in the presence of positively charged residues in its immediate surroundings (37). This latter property of PA is expected to result in a tighter docking to the binding site compared to PG species, which obviously are unable to become dianionic (38). A higher stabilizing effect of PA over PG on the stability and folding of KcsA was also reported using a different experimental approach (39).

Long-chain alkyl sulfates, despite being simpler amphiphiles than anionic phospholipids, caused almost identical increases in the protein’s t_m , suggesting that they also bind to the same nonannular sites, although with a lower affinity. The latter could be explained by the decreased hydrophobic interaction of the simpler alkyl hydrocarbon chain, compared to the double-tailed, longer phospholipids. This would be similar to the report on the decreased binding of lyso derivatives of cardiolipins to nonannular sites of cytochrome oxidase (40). Interestingly, the changes in the enthalpy in the presence of alkyl sulfates with increasing chain length suggest an extensive interaction between the amphiphiles and KcsA in the denatured state. This indicates that the binding site survives to some extent the global loss of structure associated with thermal denaturation. This is not too surprising. The thermally denatured state generally contains a residual amount of structure, and this is likely to be particularly pronounced for membrane proteins, whose hydrophobic regions are not well solvated by water. For instance, a recent study has shown a high level of structure in the SDS-denatured state of the seven-transmembrane helix protein bacteriorhodopsin, with a complete breakdown of one helix and partial breakdown of a second, but

essentially complete retention of the remaining five helices (41). This seems also consistent with the previous finding that DOPG also remained bound to dissociated, monomeric KcsA according to a mass spectrometry study (6).

The similarities between the effects of long-chain alkyl sulfates and anionic phospholipids on the protein stability may be rationalized by local docking of these molecules on the high-resolution structure of the KcsA protein. Figure 5 shows three critical interaction domains revealed from the docking model, which are contributed by residues belonging to adjacent subunits and therefore expected to specifically stabilize the tetrameric KcsA: (i) the positively charged protein surface, where R89 from one subunit and R64 and T61 from the adjacent subunit hydrogen bond to the polar headgroups of either the anionic phospholipids or the alkyl sulfates, (ii) the gorge formed by L86 and P63, defining a narrow entrance for the alkyl or acyl chains to go into the groove characteristic of the nonannular lipid binding site in this protein, and (iii) a hydrophobic pocket formed by different residues from the M2 transmembrane segment of a subunit and from the pore helix of the adjacent subunit. This hydrophobic pocket can be accessed effectively either by the *sn*-1 acyl chain of the anionic phospholipids or by the carbon chain of the longer alkyl sulfates, and its importance has been envisioned from the experiments using different chain-length ligands. For instance, as there are no differences in the effects on thermal stability caused by dimyristoyl or dioleoyl derivatives of either PA and PG, it seems reasonable to conclude that interactions involving C15–C18 at the methyl end of the chain (i.e., those arising from V93, V94, or V97) do not contribute significantly to the observed protein stabilization. Likewise, because alkyl sulfates shorter than eight carbon atoms do not have any effect on KcsA thermal stability, it may be assumed that the more relevant interactions with the protein are those established from C9 to C12 in the SDS molecule (or up to C14 in the tetradecyl derivative). These two arguments highlight the importance of the upper (nearest to the extracellular surface) part of the hydrophobic pocket referred above as the common denominator of all relevant interactions with the nonannular sites reported here. Occupancy of such a pocket, as well as that of the narrow entrance made by the preceding gorge, which are both intersubunit regions, seems to be a major factor in holding together adjacent subunits, leading to the stabilization of the tetrameric structure. A corollary from the above is that the use of the SDS–PAGE technique to evaluate KcsA stability should be approached with caution due to the stabilizing effects of the alkyl sulfate reported here. In the case of the phospholipids, an additional contribution to tetramer stability is expected to arise from the hydrophobic interaction of the *sn*-2 acyl chain with the protein transmembrane surface, which involves again residues belonging to the two adjacent subunits. This additional contribution to binding explains the larger efficiency of anionic phospholipids compared to alkyl sulfates in increasing KcsA stability. In all cases, the hydrophobic interactions should also be complemented by a minor contribution to tetramer stability from the few hydrogen bonds established between the polar head of the ligands and the positively charged surface of the protein.

REFERENCES

1. Doyle, D. A., Morais Cabral, J., Pfuetzner, R. A., Kuo, A., Gulbis, J. M., Cohen, S. L., Chait, B. T., and MacKinnon, R. (1998) The structure of the potassium channel: molecular basis of K^+ conduction and selectivity. *Science* 280, 69–77.

2. Zhou, Y., Morais-Cabral, J. H., Kaufman, A., and MacKinnon, R. (2001) Chemistry of ion coordination and hydration revealed by a K⁺ channel-Fab complex at 2.0 Å resolution. *Nature* *414*, 43–48.
3. Uysal, S., Vasquez, V., Tereshko, V., Esaki, K., Fellouse, F. A., Sidhu, S. S., Koide, S., Perozo, E., and Kossiakoff, A. (2009) Crystal structure of full-length KcsA in its closed conformation. *Proc. Natl. Acad. Sci. U.S.A.* *106*, 6644–6649.
4. Schrempf, H., Schmidt, O., Kummerlen, R., Hinnah, S., Muller, D., Betzler, M., Steinkamp, T., and Wagner, R. (1995) A prokaryotic potassium ion channel with two predicted transmembrane segments from *Streptomyces lividans*. *EMBO J.* *14*, 5170–5178.
5. Valiyaveetil, F. I., Zhou, Y., and MacKinnon, R. (2002) Lipids in the structure, folding, and function of the KcsA K⁺ channel. *Biochemistry* *41*, 10771–10777.
6. Demmers, J. A., van Dalen, A., de Kruijff, B., Heck, A. J., and Killian, J. A. (2003) Interaction of the K⁺ channel KcsA with membrane phospholipids as studied by ESI mass spectrometry. *FEBS Lett.* *541*, 28–32.
7. Deol, S. S., Domene, C., Bond, P. J., and Sansom, M. S. (2006) Anionic phospholipid interactions with the potassium channel KcsA: simulation studies. *Biophys. J.* *90*, 822–830.
8. Lee, A. G. (2003) Lipid-protein interactions in biological membranes: a structural perspective. *Biochim. Biophys. Acta* *1612*, 1–40.
9. Alvis, S. J., Williamson, I. M., East, J. M., and Lee, A. G. (2003) Interactions of anionic phospholipids and phosphatidylethanolamine with the potassium channel KcsA. *Biophys. J.* *85*, 3828–3838.
10. Marius, P., Alvis, S. J., East, J. M., and Lee, A. G. (2005) The interfacial lipid binding site on the potassium channel KcsA is specific for anionic phospholipids. *Biophys. J.* *89*, 4081–4089.
11. Opekarova, M., and Tanner, W. (2003) Specific lipid requirements of membrane proteins—a putative bottleneck in heterologous expression. *Biochim. Biophys. Acta* *1610*, 11–22.
12. Lee, A. G. (2004) How lipids affect the activities of integral membrane proteins. *Biochim. Biophys. Acta* *1666*, 62–87.
13. Heginbotham, L., Kolmakova-Partensky, L., and Miller, C. (1998) Functional reconstitution of a prokaryotic K⁺ channel. *J. Gen. Physiol.* *111*, 741–749.
14. Marius, P., Zagnoni, M., Sandison, M. E., East, J. M., Morgan, H., and Lee, A. G. (2008) Binding of anionic lipids to at least three nonannular sites on the potassium channel KcsA is required for channel opening. *Biophys. J.* *94*, 1689–1698.
15. Barrera, F. N., Renart, M. L., Poveda, J. A., de Kruijff, B., Killian, J. A., and Gonzalez-Ros, J. M. (2008) Protein self-assembly and lipid binding in the folding of the potassium channel KcsA. *Biochemistry* *47*, 2123–2133.
16. van Dalen, A., Hegger, S., Killian, J. A., and de Kruijff, B. (2002) Influence of lipids on membrane assembly and stability of the potassium channel KcsA. *FEBS Lett.* *525*, 33–38.
17. Molina, M. L., Encinar, J. A., Barrera, F. N., Fernandez-Ballester, G., Riquelme, G., and Gonzalez-Ros, J. M. (2004) Influence of C-terminal protein domains and protein-lipid interactions on tetramerization and stability of the potassium channel KcsA. *Biochemistry* *43*, 14924–14931.
18. Sehgal, P., and Otzen, D. E. (2006) Thermodynamics of unfolding of an integral membrane protein in mixed micelles. *Protein Sci.* *15*, 890–899.
19. Kelly, S. M., Jess, T. J., and Price, N. C. (2005) How to study proteins by circular dichroism. *Biochim. Biophys. Acta* *1751*, 119–139.
20. Barrera, F. N., Renart, M. L., Molina, M. L., Poveda, J. A., Encinar, J. A., Fernandez, A. M., Neira, J. L., and Gonzalez-Ros, J. M. (2005) Unfolding and refolding in vitro of a tetrameric, alpha-helical membrane protein: the prokaryotic potassium channel KcsA. *Biochemistry* *44*, 14344–14352.
21. Krieger, E., Koraimann, G., and Vriend, G. (2002) Increasing the precision of comparative models with YASARA NOVA—a self-parameterizing force field. *Proteins* *47*, 393–402.
22. Krieger, E., Darden, T., Nabuurs, S. B., Finkelstein, A., and Vriend, G. (2004) Making optimal use of empirical energy functions: force-field parameterization in crystal space. *Proteins* *57*, 678–683.
23. Wang, J., Cieplak, P., and Kollman, P. A. (2000) How well does a restrained electrostatic potential (RESP) model perform in calculating conformational energies of organic and biological molecules? *J. Comput. Chem.* *21*, 1049–1074.
24. Morris, G. M., Huey, R., and Olson, A. J. (2008) Using AutoDock for ligand-receptor docking. *Curr. Protoc. Bioinf.* *8* (Unit 8), 14.
25. Schmid, F. X. (1997) Optical spectroscopy to characterize protein conformation, in *Protein Structure: A Practical Approach* (Creighton, T. E., Ed.) 2nd ed., pp 261–298, IRL Press, Oxford.
26. Sehgal, P., Mogensen, J. E., and Otzen, D. E. (2005) Using micellar mole fractions to assess membrane protein stability in mixed micelles. *Biochim. Biophys. Acta* *1716*, 59–68.
27. Otzen, D. E., Miron, S., Akke, M., and Oliveberg, M. (2004) Transient aggregation and stable dimerization induced by introducing an Alzheimer sequence into a water-soluble protein. *Biochemistry* *43*, 12964–12978.
28. Krishnan, M. N., Bingham, J. P., Lee, S. H., Trombley, P., and Moczydlowski, E. (2005) Functional role and affinity of inorganic cations in stabilizing the tetrameric structure of the KcsA K⁺ channel. *J. Gen. Physiol.* *126*, 271–283.
29. Renart, M. L., Barrera, F. N., Molina, M. L., Encinar, J. A., Poveda, J. A., Fernandez, A. M., Gomez, J., and Gonzalez-Ros, J. M. (2006) Effects of conducting and blocking ions on the structure and stability of the potassium channel KcsA. *J. Biol. Chem.* *281*, 29905–29915.
30. Chen, X. W., and Matthews, C. R. (1994) Thermodynamic properties of the transition state for the rate-limiting step in the folding of the alpha subunit of tryptophan synthase. *Biochemistry* *33*, 6356–6362.
31. Fersht, A. R. (1999) *Structure and mechanism in protein science. A guide to enzyme catalysis and protein folding.*, 3rd ed., Freeman, New York.
32. Chandler, D. (2005) Interfaces and the driving force of hydrophobic assembly. *Nature* *437*, 640–647.
33. Gallagher, K. R., and Sharp, K. A. (2003) A new angle on heat capacity changes in hydrophobic solvation. *J. Am. Chem. Soc.* *125*, 9853–9860.
34. Simmonds, A. C., East, J. M., Jones, O. T., Rooney, E. K., McWhirter, J., and Lee, A. G. (1982) Annular and non-annular binding sites on the (Ca²⁺ + Mg²⁺)-ATPase. *Biochim. Biophys. Acta* *693*, 398–406.
35. de Foresta, B., le Maire, M., Orlowski, S., Champeil, P., Lund, S., Moller, J. V., Michelangeli, F., and Lee, A. G. (1989) Membrane solubilization by detergent: use of brominated phospholipids to evaluate the detergent-induced changes in Ca²⁺-ATPase/lipid interaction. *Biochemistry* *28*, 2558–2567.
36. Molina, M. L., Barrera, F. N., Fernandez, A. M., Poveda, J. A., Renart, M. L., Encinar, J. A., Riquelme, G., and Gonzalez-Ros, J. M. (2006) Clustering and coupled gating modulate the activity in KcsA, a potassium channel model. *J. Biol. Chem.* *281*, 18837–18848.
37. Kooijman, E. E., Tieleman, D. P., Testerink, C., Munnik, T., Rijkers, D. T., Burger, K. N., and de Kruijff, B. (2007) An electrostatic/hydrogen bond switch as the basis for the specific interaction of phosphatidic acid with proteins. *J. Biol. Chem.* *282*, 11356–11364.
38. Kooijman, E. E., and Burger, K. N. (2009) Biophysics and function of phosphatidic acid: a molecular perspective. *Biochim. Biophys. Acta* *1791*, 881–888.
39. Raja, M., Spelbrink, R. E., de Kruijff, B., and Killian, J. A. (2007) Phosphatidic acid plays a special role in stabilizing and folding of the tetrameric potassium channel KcsA. *FEBS Lett.* *581*, 5715–5722.
40. Robinson, N. C., Zborowski, J., and Talbert, L. H. (1990) Cardiolipin-depleted bovine heart cytochrome *c* oxidase: binding stoichiometry and affinity for cardiolipin derivatives. *Biochemistry* *29*, 8962–8969.
41. Pan, Y., Brown, L., and Konermann, L. (2009) Mapping the structure of an integral membrane protein under semi-denaturing conditions by laser-induced oxidative labeling and mass spectrometry. *J. Mol. Biol.* *394*, 968–981.